Photodissociation Pathways and Recombination Kinetics for Gas-Phase $Mn_2(CO)_{10}$

T. A. Seder,[†] Stephen P. Church,[‡] and Eric Weitz*

Contribution from the Department of Chemistry, Northwestern University, Evanston, Illinois 60201. *Received April 28, 1986*

Abstract: Both $Mn(CO)_5$ and $Mn_2(CO)_9$ are observed following gas-phase photolysis of $Mn_2(CO)_{10}$. The $Mn(CO)_5/Mn_2(CO)_9$ ratio can be shifted to favor formation of $Mn_2(CO)_9$ by increasing the photolysis energy from 351 to 248 to 193 nm. $Mn(CO)_5$ is formed with significant amounts of internal excitation. Further, as the photolysis energy increases, additional photoproducts are produced which are tentatively assigned as predominantly $Mn_2(CO)_x$ species ($x < 9$). IR absorptions of both $Mn(CO)_5$ and $Mn_2(CO)_9$ have been recorded and assigned in the range $\sim$2050 to $\sim$1750 cm^{-1}. The rate constant for the reaction of two $Mn(CO)_5$ radicals to form $Mn_2(CO)_{10}$ has been measured and found to be near gas kinetic. The rate constant for the reaction of $Mn_2(CO)_9$ with CO to form $Mn_2(CO)_{10}$ has been determined to be $(2.4 \pm 0.8) \times 10^6$ L mol^{-1} s^{-1}.

The photochemistry of organometallic complexes is an area of vigorous current research.[1] $Mn_2(CO)_{10}$ represents a particularly interesting system for study since the bonding in this molecule is such that two primary photochemical events leading to the generation of neutral fragments can be envisioned. One fragmentation pathway involves heterolytic cleavage of a manganese–carbon bond, while the other pathway involves cleavage of the manganese–manganese bond. Reports of dissociation via each of these pathways appear in the literature.[1-17]

One of the photochemical decomposition pathways reported involves formation of $Mn(CO)_5$ via

$$Mn_2(CO)_{10} \xrightarrow{h\nu} 2Mn(CO)_5 \qquad (1)$$

It has been fairly well-established that the electronic transition responsible for generating the 17-electron pentacarbonyl breaks the metal–metal bond by promoting an electron from the σ bonding orbital to the σ antibonding orbital,[4] i.e., $\sigma(M-M) \rightarrow \sigma^*(M-M)$. By using a combination of ^{13}CO enrichment and IR spectroscopy Church et al.[9] showed that the $Mn(CO)_5$ radical adopts the predicted[16] square pyramidal, C_{4v} geometry. In a CO matrix the pentacarbonyl is reported to absorb at 1988 cm^{-1} and 1978 cm^{-1}.[9] The higher frequency absorption corresponds to the E mode, while the lower frequency corresponds to a vibration of A_1 symmetry. In solution the decay of an infrared absorption of $Mn(CO)_5$ obeys second-order kinetics, compatible with the radical–radical recombination reaction

$$2Mn(CO)_5 \xrightarrow{k_1} Mn_2(CO)_{10} \qquad (2)$$

The value for k_1 of 1×10^9 L mol^{-1} s^{-1} for reaction 2 in *n*-heptane indicates that the kinetic process approaches the diffusion limit.[11]

In addition to process 1, a second photochemical pathway has been observed upon UV photolysis of $Mn_2(CO)_{10}$.[17] Hepp and Wrighton[7a] report that dissociative CO loss via

$$Mn_2(CO)_{10} \xrightarrow{h\nu} Mn_2(CO)_9 + CO \qquad (3)$$

accounts for the fate of $\sim$30% of the alkane matrix isolated $Mn_2(CO)_{10}$ molecules which have absorbed UV radiation. The matrix trapped products, $Mn_2(CO)_9$ and free CO, have been detected through their infrared absorptions. $Mn_2(CO)_9$ exhibits multiple infrared absorptions in a 77 K 3-methylpentane matrix[7a] including one at 1760 cm^{-1}. This 1760-cm^{-1} band signifies that $Mn_2(CO)_9$ contains a bridging CO moiety. Elegant experiments in Ar matrices at 12 K involving the use of polarized light have shown that the CO linkage across the Mn–Mn bond in $Mn_2(CO)_9$ is semibridging[7b] in nature. This 1760-cm^{-1} bridging band has also been observed following UV photolysis of solution phase $Mn_2(CO)_{10}$ by Church et al.[11] In addition to the prominent bridging band, absorptions observed at 2058, 2022, 2008, 1996, and 1968 cm^{-1} have also been attributed to $Mn_2(CO)_9$ (in C_7H_{16} solution). These bands display pseudo-first-ordered kinetics upon addition of CO, indicating occurrence of the process

$$Mn_2(CO)_9 + CO \xrightarrow{k_2} Mn_2(CO)_{10} \qquad (4)$$

k_2 has been measured as 2.7×10^6 L mol^{-1} s^{-1} (C_7H_{16} solvent).[11]

Dissociative CO loss upon UV photolysis of $Mn_2(CO)_{10}$ has also been reported by several other groups.[12,13,17b] Vaida et al.[12] have recorded the visible absorption spectrum of the products of 355-nm photolysis of ethanol solutions of $Mn_2(CO)_{10}$ and report that two transient absorptions (780 and 480 nm) are observed. Yasufuku et al. detected solution phase $Mn(CO)_5$ and $Mn_2(CO)_9$ through their transient visible absorptions and noted a dependence of the relative yield upon photolysis wavelength. Defining Y_1 and Y_2 as the quantum yield of $Mn(CO)_5$ and $Mn_2(CO)_9$, respectively, they report that the ratio Y_1/Y_2 varies from 0.21 for 266-nm photolysis to 0.74 for 355-nm photolysis.

Relatively few photochemical studies have been performed on the gas-phase $Mn_2(CO)_{10}$. Freedman and Bersohn[14] have studied the photodissociation ($\lambda \sim 300$ nm) dynamics of molecular beams of $M_2(CO)_{10}$ (M = Re or Mn). Through their measurements of the effect of polarization of incident light upon the angular distribution of photogenerated $Mn(CO)_5$ fragments, they have set an upper limit of several picoseconds on the lifetime of the $Mn_2(CO)_{10}$ excited state. Further, their TOF mass spectra indicate the presence of only $Mn(CO)_5$. However, Leopold and

[†] Present address: General Motors Research Laboratories, Physical Chemistry Department, Warren, MI 48090.

[‡] Present address: Max Planck Institut für Strahlenchemie, D-4330 Mülheim a.d. Ruhr, West Germany.

(1) Geoffroy, G. L.; Wrighton, M. S. *Organometallic Photochemistry*; Academic: New York, 1979.
(2) Coville, N. J.; Stolzenberg, A. M.; Muetterties, E. L. *J. Am. Chem. Soc.* **1983**, *105*, 2499.
(3) For a recent review, see: Meyer, T. J.; Casper, J. V. *Chem. Rev.* **1985**, *85*, 187.
(4) Levenson, R. A.; Gray, H. B.; Ceasar, G. P. *J. Am. Chem. Soc.* **1970**, *92*, 3653.
(5) Hughey, J. L.; Anderson, C. P.; Meyer, T. J. *J. Organomet. Chem.* **1977**, *125*, C49.
(6) Fox, A.; Poë, A. *J. Am. Chem Soc.* **1980**, *102*, 2497.
(7) (a) Hepp, A. F.; Wrighton, M. S. *J. Am. Chem. Soc.* **1983**, *105*, 5934. (b) Dunkin, I. R.; Härtner, P.; Shields, C. J. *J. Am. Chem. Soc.* **1984**, *106*, 7248.
(8) Bray, R. G.; Seidler, P. F., Jr.; Gethner, J. S.; Woodin, R. L. *J. Am. Chem. Soc.* **1986**, *108*, 1312.
(9) Church, S. P.; Poliakoff, M.; Timney, J. A.; Turner, J. J. *J. Am. Chem. Soc.* **1981**, *103*, 7515.
(10) Poliakoff, M. *Chem. Soc. Rev.* **1978**, *2*, 527.
(11) Church, S. P.; Hermann, H.; Grevels, F.; Schaffner, K. *J. Chem. Soc., Chem. Commun.* **1984**, 785 and references therein.
(12) Rothberg, L. J.; Cooper, N. J.; Peters, K. S.; Vaida, V. *J. Am. Chem. Soc.* **1982**, *104*, 3536.
(13) Yasufuku, K.; Kobayashi, T.; Iwai, J.; Yesaka, H.; Noda, H.; Ohtani, H. *Coord. Chem. Res.* **1985**, *64*, 1.
(14) Freedman, A.; Bersohn, R. *J. Am. Chem. Soc.* **1978**, *100*, 4116.
(15) Leopold, D. G.; Vaida, V. *J. Am. Chem. Soc.* **1984**, *106*, 3720.
(16) Burdett, J. K. *J. Chem. Soc. Faraday Trans. 2* **1974**, *70*, 1599.
(17) (a) Walker, H. W.; Herrick, R. S.; Olsen, R. J.; Brown, T. L. *Inorg. Chem.* **1984**, *23*, 3748. (b) Herrick, R. S.; Brown, T. L. *Ibid.* **1984**, 4550.

0002-7863/86/1508-7518$01.50/0

Vaida[15] report the presence of Mn_2 ion signals in the TOF mass spectra which utilized 422-nm MPI detection subsequent to 337 nm photolysis of molecular beams of $Mn_2(CO)_{10}$. A further interesting result of their studies is that no carbonyl containing species were detected. This could imply that the Mn metal–metal bond strengthens as the $Mn_2(CO)_x$ fragment is decarbonylated. Recently the observation of Freedman and Bersohn[14] that nascent photogenerated $Mn(CO)_5$ radicals are in high lying vibrational states has been confirmed by Bray et al.[8] These researchers have measured the vibrational relaxation rate of $Mn(CO)_5$ with various collision partners.

The results of the studies mentioned above form a very important base of information which is used in the analysis of our gas-phase studies of $Mn_2(CO)_{10}$ photolysis. In the remainder of this article, experiments designed to generate and detect $Mn(CO)_5$ and $Mn_2(CO)_9$ will be described and discussed. Following identification of the primary photofragments through their infrared absorptions, the kinetics of the reaction of these fragments is discussed. In addition, preliminary experiments on the wavelength dependence of the photolytic process are reported.

Experimental Section

The apparatus used to record the time resolved spectra of transient unsaturated metal carbonyls has been described in detail elsewhere.[18] Briefly, all of the sample gases, except $Mn_2(CO)_{10}$, are passed through a flow cell at a rate such that the cell volume is completely replenished during the period between photolysis pulses (1 s). A constant steady-state pressure of $Mn_2(CO)_{10}$ is achieved by placing a small amount of the solid into the cell. Controlled and variable amounts of CO and/or Ar can be added to the cell by means of Tylan computer controllable flow controllers. Approximately 2 mtorr of the sublimed $Mn_2(CO)_{10}$ is photolyzed by the 6 mJ/cm^2, 15 ns pulse provided by a Questek 2000 excimer laser. In some experiments the pressure of photolyzed $Mn_2(CO)_{10}$ was increased to ~10 mtorr by warming the cell to 50 °C.

The transient species produced by UV photolysis were monitored via the output of a home-built, liquid nitrogen cooled, line tunable carbon monoxide laser. The CW infrared beam, after making a double pass through the flow cell, is dispersed to fill the entire area of an indium antimonide detector. The output of the detector is amplified (×100 Perry 070/40), fed through a unity gain buffer amplifier (Perry), and ultimately digitized by a Biomation 8100 waveform recorder. Typically, 64 waveforms are averaged via simple addition by a Nicolet 1170 signal averager. The signals are stored on a Nova/4 microcomputer, which is in communication with a Harris super-minicomputer. The measured response time of the detection system is 35 ns.

Time resolved infrared spectra of the transient species are constructed from transient waveforms acquired at probe frequencies within the carbonyl stretch region, by a computer program which joins together the amplitude of each waveform at a particular time.

$Mn_2(CO)_{10}$ (95+% pure) was obtained from Alpha Chemical Co. and used without further purification since it was sublimed in situ. Ar (99.99+% purity) and CO (99.99+% purity) were obtained from Matheson and used without further purification.

Results and Discussion

XeF Laser Photolysis. The transient infrared absorption spectrum obtained 25 μs after XeF laser (351-nm) photolysis of 2 mtorr of $Mn_2(CO)_{10}$ in the presence of 15 torr of Ar buffer is shown in Figure 1. The positive features in this figure correspond to absorptions of photolytically generated species, while the negative features represent photolytic depletion of $Mn_2(CO)_{10}$. The infrared absorption bands of $Mn_2(CO)_{10}$ in Figure 1 can be identified via comparison with the bands which appear in the normal infrared spectrum. An FTIR spectrum of gas-phase $Mn_2(CO)_{10}$ is shown in Figure 2. The absorptions of the D_{4d} $Mn_2(CO)_{10}$ molecule at 2053, 2026, and 1993 cm^{-1}, appearing in a relative intensity ratio of 1.7:5.1:1, have been previously determined to belong to bands of B_2, E_1, and B_2 symmetry, respectively.[4] While the 2053- and 2026-cm^{-1} bands clearly appear as negative features in the transient spectrum (Figure 1), the 1993-cm^{-1} band *appears* to be absent. Its apparent absence is due to an overlap with the intense positive absorption centered at 2000 cm^{-1}.

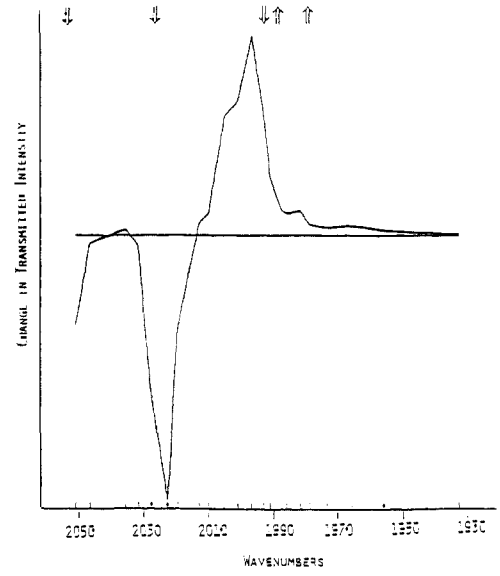

Figure 1. Transient infrared absorption spectrum generated via XeF laser photolysis of $Mn_2(CO)_{10}$. Downward pointing arrows denote the absorption frequencies of gas-phase $Mn_2(CO)_{10}$, while upward pointing arrows denote that of matrix-isolated $Mn(CO)_5$. The spectrum was recorded 25 μs following photolysis of 2 mtorr of $Mn_2(CO)_{10}$ in the presence of 15 torr of Argon.

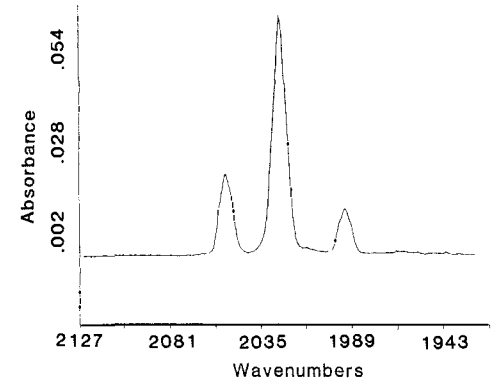

Figure 2. Fourier transform infrared absorption spectrum of $Mn_2(CO)_{10}$ (g). $Mn_2(CO)_{10}$ was at its vapor pressure at 294 ± 1 K in a 10-cm cell. The resolution of the spectrum is 2 cm^{-1}.

As mentioned earlier, matrix isolated $Mn(CO)_5$ adopts the predicted[16] C_{4v} geometry and exhibits infrared absorptions at 1988 cm^{-1} (E) and 1978 cm^{-1} (A_1).[9] In accord with these data, and taking into account the expected shift between matrix and gas-phase absorptions,[19] the intense positive absorption at 2000 cm^{-1} is assigned to an overlap of the E and A_1 vibrations of gas-phase square pyramidal $Mn(CO)_5$. The emission lines of the CO probe laser limits the resolution of the spectrum in Figure 1 to approximately 4 cm^{-1}. Since gas-phase metal–carbonyls exhibit rather broad absorption bands, it is not surprising that the E and A_1 vibrational bands of $Mn(CO)_5$ are not resolved. Further complicating the situation is the existence in the 2000-cm^{-1} region of the lower frequency B_2 vibrational band of $Mn_2(CO)_{10}$. This overlap of the E and A_1 absorption bands is similar to what has been observed in hydrocarbon solutions where an infrared absorption band observed at 1988 cm^{-1} following UV photolysis of $Mn_2(CO)_{10}$ has been assigned to the unresolved E and A_1 vibrational bands of the C_{4v} pentacarbonyl.[11]

Since XeF laser excitation inputs 82 kcal/mol and the Mn–Mn bond is estimated to be ~36 kcal/mol, it might be expected that the $Mn(CO)_5$ fragments generated in these experiments would possess a high degree of internal excitation. Further, based on Freedman and Bersohn's[14] measurement of the energy distribution

(18) Seder, T. A.; Church, S. P.; Weitz, E. *J. Am. Chem. Soc.* **1986**, *108*, 4721.

(19) *Vibrational Spectroscopy of Trapped Species*; Hallam, H. E., Ed.; Wiley: New York, 1973.

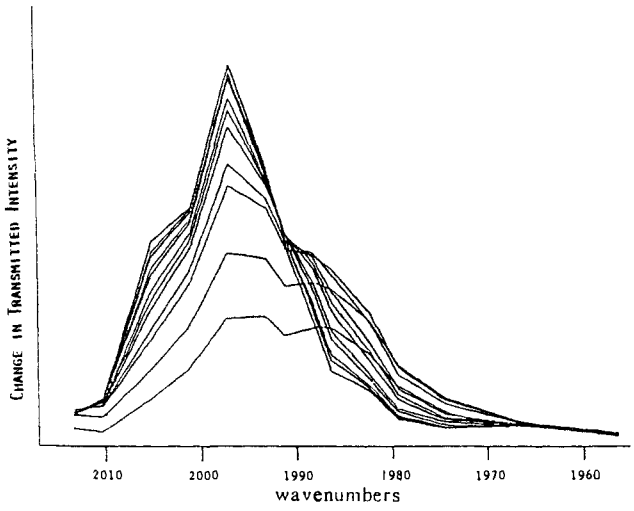

Figure 3. Transient time resolved infrared absorption spectrum of the $Mn(CO)_5$ species generated via XeF laser photolysis of $Mn_2(CO)_{10}$. The ordinate is an arbitrary linear scale. The 1993-cm^{-1} band of $Mn_2(CO)_{10}$ has been subtracted from the spectrum. The spectrum depicts the growth of the $Mn(CO)_5$ absorption and contains 10 equally spaced transients with a spacing of 100 ns between transients.

in the fragments produced by photodissociation of $Re_2(CO)_{10}$ in a molecular beam, it seems to be reasonable to expect that most of the internal energy would appear as vibrational excitation. They report that $^2/_3$ of the available energy appears as internal energy[14] and that most of that energy is likely in vibrational modes of the photofragments. As mentioned earlier, Bray et al.[8] have recently confirmed that photogenerated $Mn(CO)_5$ retains a significant amount of the input energy as vibrational motion. They estimate an average vibrational excess energy of 13–16 kcal/mol for each $Mn(CO)_5$ fragment.

One can easily visualize how the dynamics of this dissociative event can generate fragments having high levels of vibrational excitation. A possible scenario whose general picture was suggested by Freedman and Bersohn is as follows: 351-nm radiation excites the $\sigma \rightarrow \sigma^*$ transition, formally reducing the order of the Mn–Mn bond to zero. This can be viewed as the switching on of a repulsive potential between the manganese atoms, causing them to fly apart with very little torsional (rotational) motion. Initially, the CO ligands are spectators to this impulsive event. As the Mn–Mn bond lengthens, the $Mn–CO_{axial}$ bond length and the $CO_{axial}–Mn–CO_{equatorial}$ bond angle change. This will lead to vibrational excitation of the Mn–CO stretching and bending modes. Since intramolecular vibrational transfer is rapid,[20] the above dynamical event will lead to an increase in the "vibrational temperature" of the molecule.[21] Experimentally, this manifests itself by broadened vibrational bands which are shifted to lower energy.[19,22] Following formation, these vibrationally excited species would be expected to relax via collisions with other molecules in the flow cell via the process

$$Mn(CO)_5^* + M \rightarrow Mn(CO)_5 + M$$

This should result in a pressure dependent narrowing and shifting to higher frequency of the absorption bands of the $Mn(CO)_5$ moiety. This is, indeed, found to occur. The evolution of the 2000-cm^{-1} absorption of $Mn(CO)_5$ is, however, obscured by the overlapping, 1993-cm^{-1} band of $Mn_2(CO)_{10}$. The 1993-cm^{-1} band can be subtracted from the spectrum since its intensity relative to the 2026-cm^{-1} band is known, and both the intensity and

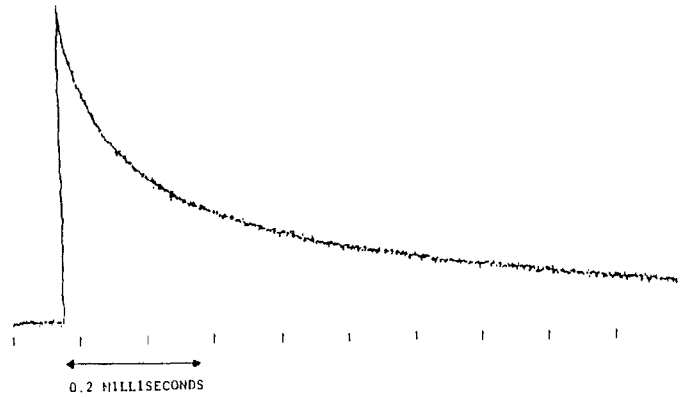

Figure 4. Temporal behavior of the $Mn(CO)_5$ absorption at 2004 cm^{-1}. The ordinate is an arbitrary linear scale, and the abscissa is in units of time as indicated. The length of the arrow on the abscissa is 0.2 ms giving a full time base for the signal of ~1.0 ms.

temporal behavior of the 2026-cm^{-1} band are known. The transient time resolved infrared absorption spectrum of the XeF laser generated $Mn(CO)_5$ fragment is shown in Figure 3 with the interferring parent band subtracted from this spectrum. (Note that the subtraction is not perfect, and remnants of the interferring band appear as a "dip" at 1993 cm^{-1}.)

Further evidence that the 2000-cm^{-1} band is that of $Mn(CO)_5$ can be obtained by examining the decay kinetics of this absorption. The gas-phase transient waveform of $Mn(CO)_5$ at 2004 cm^{-1}, in the presence of 15 torr of Ar, is displayed in Figure 4. The decay clearly follows a second-order rate law and is consistent with the $Mn_2(CO)_{10}$ reformation pathway

$$2Mn(CO)_5 \xrightarrow{k_1} Mn_2(CO)_{10} \qquad (2)$$

From I/I_0 measurements, an assumed infrared extinction coefficient for $Mn(CO)_5$, and the plot of $1/I - 1/I_0$ against time (Figure 5), the bimolecular rate constant, k_1, has been calculated to be $(4.5 \pm 1.0) \times 10^{10}$ L mol^{-1} s^{-1} at 323 K. The error limits reflect the 95% confidence limits for the slope of the line in Figure 5 and do not include the uncertainties in the choice of ϵ. The value of ϵ used to calculate k_1 is the peak value for the E_1 mode of $Mn(CO)_5Cl$ (6560 L mol^{-1} cm^{-1}).[23] ϵ should not change significantly between $Mn(CO)_5$ and $Mn(CO)_5Cl$ since the presence of the Cl should not significantly effect the CO vibrational modes or their intensity.[11] This value of k_1 is slightly different than the value previously reported for k_1.[24] This is due to more accurate measurements of I/I_0 and a choice of ϵ which represents the best estimate possible in the absence of an actual measurement of ϵ. Though the dependence of k_1 on buffer gas pressure has not been studied in detail, no rare gas pressure dependence has been observed, and an estimate of the lifetime of the $Mn_2(CO)_{10}$ complex formed via radical recombination confirms that third body effects should be unimportant under our experimental conditions.

Interestingly, the $Mn_2(CO)_{10}$ transient absorption at 2026 cm^{-1} does not return to the original base line. Rather it approaches a new base line with second-order kinetic behavior. With an appropriate choice of the new base line (which effectively determines the percentage of parent regenerated via reaction 2 and thus the relationship between signal intensity and concentration for $Mn_2(CO)_{10}$), the rate constant for regeneration of parent can be determined as $(4.4 \pm 1.0) \times 10^{10}$ L mol^{-1} s^{-1} at 323 K, which is in very good agreement with the value of k_1 determined by monitoring $Mn(CO)_5$. Again the error limits reflect only errors in the slope of the line in Figure 5. Despite this agreement, since approximations are involved in the determination of both of these rate constants it is probably best to say that the rate constant for recombination of $Mn(CO)_5$ radicals is close to that expected for a gas-kinetic radical–radical recombination process, which would

(20) Yardley, J. T. *Introduction to Molecular Energy Transfer*; Academic: New York, 1980.
(21) Weitz, E.; Flynn, G. W. *Adv. Chem. Phys.* **1981**, *47-II*, 185.
(22) Ouderkirk, A. J.; Wermer, P.; Schultz, N. L.; Weitz, E. *J. Am. Chem. Soc.* **1983**, *105*, 3354. Ouderkirk, A. J.; Weitz, E. *J. Chem. Phys.* **1983**, *79*, 1089. Ouderkirk, A. J.; Seder, T. A.; Weitz, E. *SPIE Proceedings* **1984**, *458*, 148. Seder, T. A.; Church, S. P.; Ouderkirk, A.; Weitz, E. *J. Am Chem. Soc.* **1985**, *107*, 1432.
(23) Abel, E. W.; Butler, I. S. *Trans. Faraday Soc.* **1967**, *63*, 45.
(24) Seder, T. A.; Church, S. P.; Weitz, E. *J. Am. Chem. Soc.* **1986**, *108*, 1084.

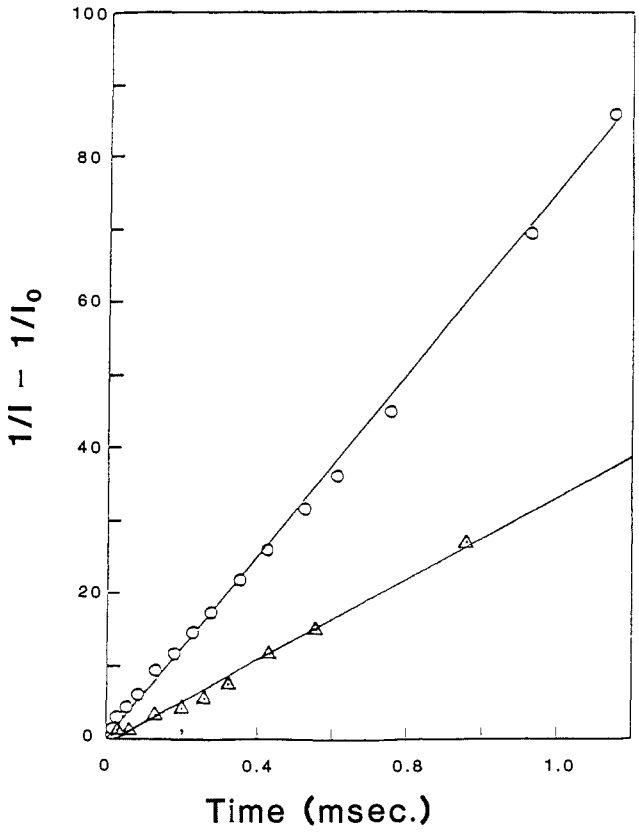

Figure 5. Plot of the second-order decay rate of the $Mn(CO)_5$ absorption against time (upper line). As described in the text a rate constant of (4.5 ± 1.0) × 10^{10} L mol^{-1} s^{-1} can be deduced from the slope of the straight line. Also shown (lower line) is a plot of the recovery of $Mn_2(CO)_{10}$. As explained in the text a rate constant of (4.4 ± 1.0) × 10^{10} L mol^{-1} s^{-1} can be deduced from the slope of this line.

have a rate constant of ~10^{11} L mol^{-1} s^{-1}. This magnitude for k_1 is consistent with liquid phase kinetic measurements, where nearly diffusion controlled rates have been measured for reaction 2.[11] Though these observations further confirm the occurrence of process 2 they also indicate that not all of the initially photolyzed $Mn_2(CO)_{10}$ is regenerated via reaction 2. This, of course, further implies that reaction 2 is *not* the only initial photochemical step. Moreover, though under our experimental conditions $Mn(CO)_5$ is inert to CO, addition of CO does lead to an increase in both the rate of regeneration and the amount of $Mn_2(CO)_{10}$ regenerated. This is compatible with the regeneration of parent via reaction of CO with a photoproduct of $Mn_2(CO)_{10}$ photolysis which is produced via CO loss. The simplest of these species is $Mn_2(CO)_9$ and by analogy with solution phase studies it might be expected to be produced in the gas phase.

There is spectroscopic evidence that $Mn_2(CO)_9$ is, indeed, generated upon 351-nm photolysis of gas-phase $Mn_2(CO)_{10}$. The transient time resolved infrared spectrum following XeF laser photolysis of $Mn_2(CO)_{10}$ in the presence of 5 torr of CO and 15 torr of Ar is displayed in Figure 6. The spectrum is depicted over a 450-μs range which has been segmented into 5 equal time intervals. From this figure it can be seen that while the $Mn(CO)_5$ absorption band has been significantly depleted, recovery of the bands of $Mn_2(CO)_{10}$ is incomplete. (Note that because of the depletion of the $Mn(CO)_5$ band, without complete regeneration of $Mn_2(CO)_{10}$, the overlapping lower frequency absorption band of $Mn_2(CO)_{10}$ now appears as a negative feature in Figure 6.) Also in Figure 6 are weak but persistent absorptions at ~2050, ~2014, and ~1980 cm^{-1}. The position of the terminal CO stretching bands of $Mn_2(CO)_9$ in an Ar matrix[7b] are marked by upward arrows in Figure 6. As the weak, persistent, gas-phase absorptions appear at the expected frequency relative to the matrix absorptions of $Mn_2(CO)_9$, we tentatively assign these absorptions to gas-phase $Mn_2(CO)_9$. These are marked by downward arrows.

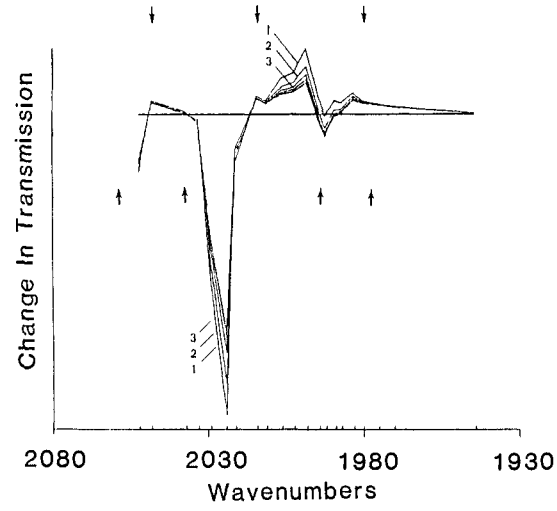

Figure 6. Transient time resolved infrared absorption spectrum generated upon XeF laser photolysis of $Mn_2(CO)_{10}$ in the presence of 5 torr CO and 15 torr Ar. The spectrum is depicted over a 450-μs range following the photolysis pulse that has been segmented into 5 equal time intervals with the first three traces being labeled in order. Upward arrows denote the frequency of absorption bands of Ar matrix isolated $Mn_2(CO)_9$. Downward arrows denote gas-phase absorptions assigned to $Mn_2(CO)_9$.

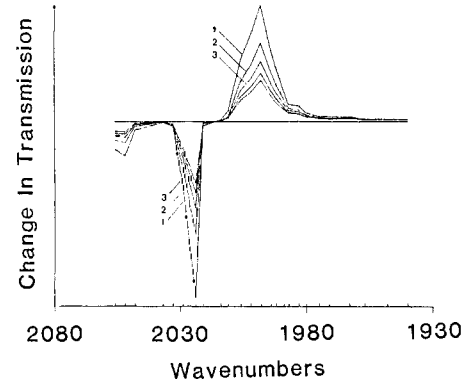

Figure 7. Transient time resolved infrared absorption spectrum generated upon XeF laser photolysis of $Mn_2(CO)_{10}$ in the presence of 85 torr CO and 15 torr Ar. The spectrum is depicted over a 450-μs range following the photolysis pulse. The range is segmented into 5 equal time intervals with the first three traces labeled in order.

The existence of a CO dependent reformation pathway is convincingly demonstrated in Figure 7. The spectrum displayed in this figure was obtained under conditions identical with those of Figure 6 except that 85 torr CO was added to the photolysis cell. Of particular interest is the fact that the weak bands that have tentatively been assigned to $Mn_2(CO)_9$ are diminished, *and* the recovery of the $Mn_2(CO)_{10}$ absorptions is more complete than in Figure 6. This strongly indicates the existence of the reaction

$$Mn_2(CO)_9 + CO \xrightarrow{k_2} Mn_2(CO)_{10} \qquad (4)$$

Recall that in condensed phases $Mn_2(CO)_9$ exhibits a 1760-cm^{-1} absorption which is attributable to the stretching mode of a bridging CO. If the structure of $Mn_2(CO)_9$ is the same in the gas phase as it is in condensed phases, the gas-phase species would typically exhibit a band at a frequency slightly higher than 1760 cm^{-1}. A thorough search of the 1800- to 1760-cm^{-1} region of the spectrum revealed no transient absorption. However, an absorption at 1745 cm^{-1} was detected (Figure 8). Though weak, this band, unlike the weak absorptions observed in the higher frequency region of the spectrum, is not affected by overlap with the intense absorptions of $Mn(CO)_5$ or $Mn_2(CO)_{10}$. Thus, the kinetic behavior of the 1745-cm^{-1} band was examined. Figure 9 displays a plot of the pseudo-first-order decay rate of the 1745-cm^{-1} band vs. pressure of added CO. From the slope of the curve, a bimolecular rate constant, k_2, of (2.4 ± 0.8) × 10^6 L mol^{-1} s^{-1} at 323 K has

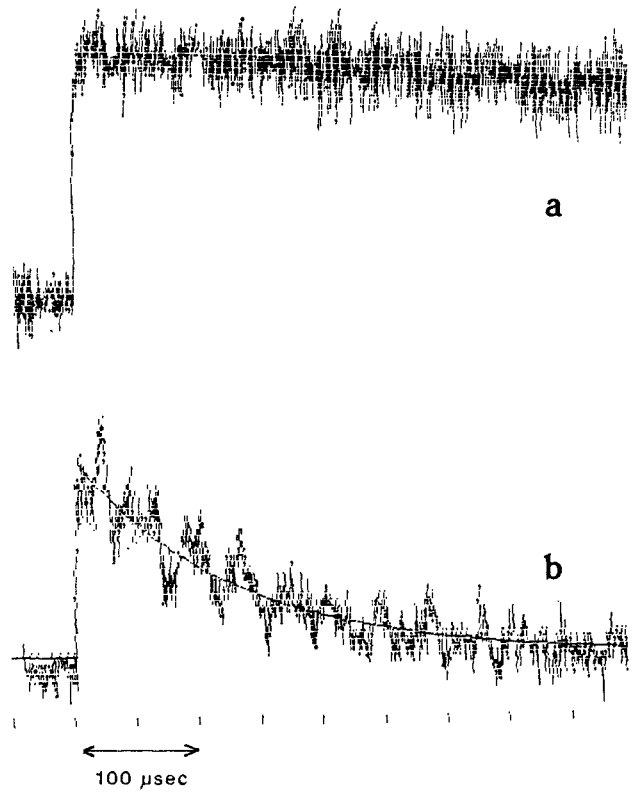

Figure 8. Temporal behavior of the $Mn_2(CO)_9$ absorption at 1745 cm^{-1}. The ordinate is arbitrary linear scale while the abscissa is in units of time as indicated. The length of the arrow on the abscissa is 100 μs giving a full timebase of ~500 μs for the signal: (a) with no added CO and (b) with 55.0 torr of added CO.

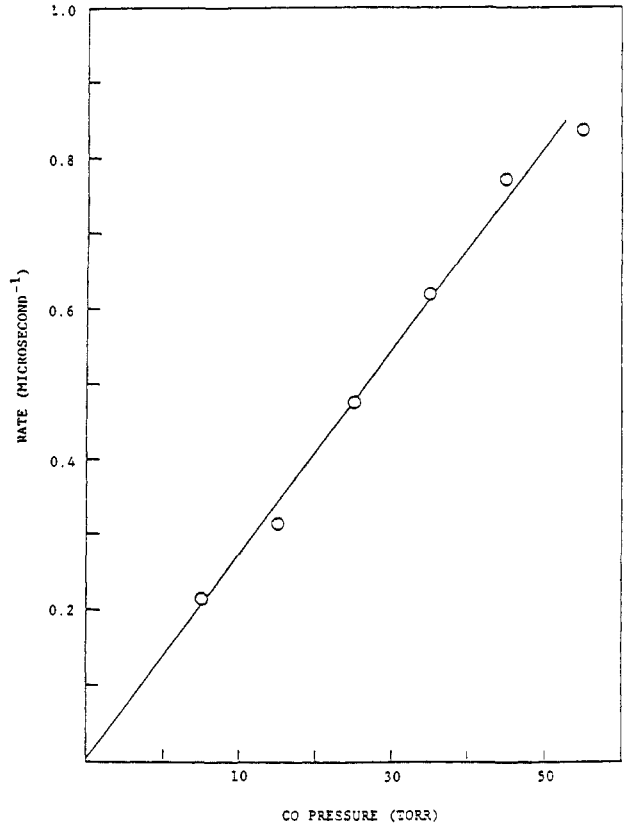

Figure 9. Plot of the pseudo-first-order decay of the 1745-cm^{-1} band of $Mn_2(CO)_9$ against pressure of added CO. The rate constant for the reaction of $Mn_2(CO)_9$ with CO is found to be $(2.4 \pm 0.8) \times 10^6$ L mol^{-1} s^{-1}.

been deduced. Interestingly, the measured rate constant for reaction 4 in solution is 2.7×10^6 L mol^{-1} s^{-1}.[11] Again, due to our experimental conditions, the reported value of k_2 is rare gas pressure independent.

As mentioned earlier, the addition of CO causes a more complete return to the original base line of the $Mn_2(CO)_{10}$ transient absorption at 2026 cm^{-1} than without added CO. Unfortunately, an analysis of the dependence of the 2026-cm^{-1} transient absorption on CO pressure is complicated by the parallel radical–radical recombination process (reaction 2) leading to regeneration of $Mn_2(CO)_{10}$. No detailed attempts were made to deconvolute the (expected) first-order, CO dependent, kinetics from the change in the 2026-cm^{-1} transient absorption. However, recall that the rate of regeneration of $Mn_2(CO)_{10}$ does increase with added CO.

In light of the above noted close agreement for k_2, with the measured rate constant for reaction 4 in solution as well as the observation of weak absorptions in the vicinity of those expected for terminal CO stretches of $Mn_2(CO)_9$, it is concluded that dissociative loss of CO occurs in the gas-phase photolysis of $Mn_2(CO)_{10}$. The 1745-cm^{-1} absorption is thus assigned to the bridging CO group of $Mn_2(CO)_9$. It is, however, interesting that this band is at *lower* frequency in the gas phase than in a matrix environment. Though not unprecedented, this is opposite the typical behavior for matrix isolated molecules.[19] The structure and/or potential energy surface for this bridging CO group may be highly sensitive to the matrix environment. However, definitive conclusions on the gas phase vs. matrix structure of $Mn_2(CO)_9$ will have to await more detailed studies in a variety of matrix media.

It is also interesting to note the large difference in rate of reaction of $Mn_2(CO)_9$ with CO vs. the rates of reaction of CO with coordinatively unsaturated Fe and Cr compounds. When a change in spin is not involved, the rate constants for these reactions are on the order of 10^{10} L mol^{-1} s^{-1}.[22,25] Even when a change of spin is involved, as in the case of the reaction of $Fe(CO)_4 + CO$,[22] the rate constant is $\sim 3 \times 10^7$ L mol^{-1} s^{-1}. An obvious explanation for the large difference in rate constant for reaction 4 vs. CO association reactions involving $Fe(CO)_x$ or $Cr(CO)_x$ species has to do with the structure of $Mn_2(CO)_9$. As mentioned above, $Mn_2(CO)_9$ contains a bridging CO which donates electron density to both Mn metal centers.[7b,11] This results in both Mn centers having 18 electrons, thus $Mn_2(CO)_9$ is coordinatively saturated. This being the case, the addition of CO to $Mn_2(CO)_9$ is effectively a displacement reaction rather than a simple association reaction. This is in accord with the observation that the rate of reaction of CO with $Mn_2(CO)_9$ was *not* accelerated in perfluoro solvent as opposed to a hydrocarbon solvent.[17b] This implies there is no easily accessible site for solvent interaction with $Mn_2(CO)_9$. Thus the semibridging CO acts as a 4-electron ligand.[26] Thus the magnitude of the rate constant for reaction 4 *is not contrary* to the emerging trend that the rate constants for simple CO addition reactions for coordinatively metal–carbonyls that conserve spin are near gas kinetic.

KrF and ArF Laser Photolysis. Some preliminary measurements on the wavelength dependence of the photofragmentation pathways of $Mn_2(CO)_{10}$ have also been performed. As noted previously, it has been found that the branching ratio for the pathway involving homolytic Mn–Mn bond cleavage to that involving dissociative CO loss can be shifted to favor CO loss by decreasing the photolysis wavelength.[13] The results of solution phase studies can be interpreted in terms of a wavelength variation in the relative probability of populating two different electronic states. It is known that there are at least two transitions ($d\pi \rightarrow \pi^*$, $M \rightarrow \pi^*$) which become more probable at shorter wavelengths.[27] A simple picture consistent with solution phase studies

(25) Fletcher, T. R.; Rosenfeld, R. N. *J. Am. Chem. Soc.* **1985**, *107*, 2203.

(26) Note that the related 32-electron stable complex $Mn_2(CO)_5(Ph_2PCH_2PPh_2)_2$ also contains a semibridging CO linkage acting as a 4-electron ligand. See: Colton, R.; Commons, C. J.; Hoskins, B. F. *J. Chem. Soc., Chem. Commun.* **1975**, 363. Commons, C. J.; Hoskins, B. F. *Aust. J. Chem.* **1975**, *28*, 1663.

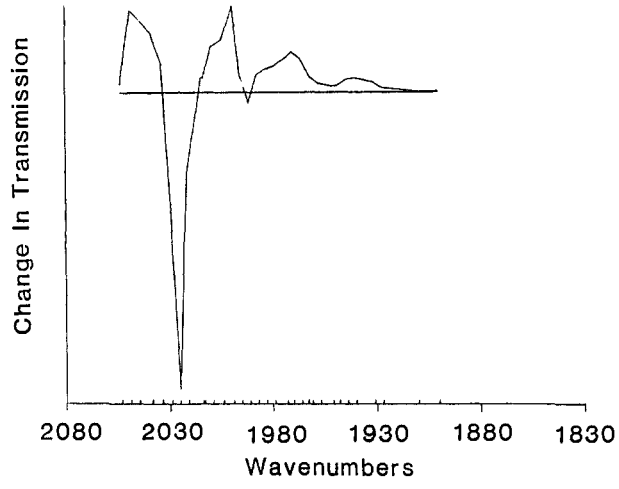

Figure 10. Transient infrared absorption spectrum for the wavelength range ~2060 to ~1900 cm^{-1} recorded 1 μs following KrF laser photolysis of $Mn_2(CO)_{10}$ in the presence of 15 torr of argon.

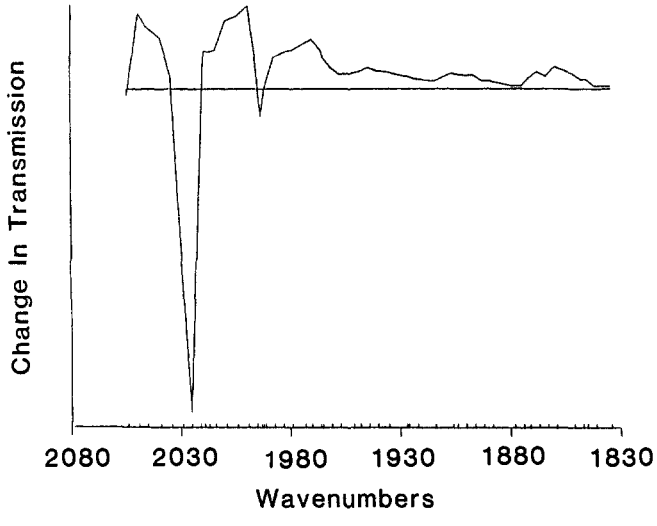

Figure 11. Transient infrared absorption spectrum for the wavelength range ~2060 to ~1830 cm^{-1} recorded 1 μs following ArF laser photolysis of $Mn_2(CO)_{10}$ in the presence of 15 torr of argon.

and an examination of the electronic spectrum of $Mn_2(CO)_{10}$ is that the photochemistry subsequent to exciting the $\sigma \rightarrow \sigma^*$ transition is that of homolytic cleavage while population of the π^* state leads to CO loss.

Since collisional energy relaxation in the primary photofragments is much faster in the solution phase than in the gas phase, gas-phase photofragments have a higher probability for unimolecular dissociation if they are formed in highly excited vibrational states. Therefore, it might be expected that in addition to $Mn(CO)_5$ and $Mn_2(CO)_9$, the infrared absorptions of the dissociation products of $Mn_2(CO)_9$ and $Mn(CO)_5$ will appear in the transient absorption spectrum following KrF- and/or ArF-laser photolysis.

The transient infrared absorption spectrum 1 μs following KrF laser photolysis of $Mn_2(CO)_{10}$ in the presence of 15 torr Ar is shown in Figure 10. By comparing the relative amplitude of the $Mn(CO)_5$ absorption (2000 cm^{-1}) to the amount of parent photolyzed in Figure 10 to that in Figure 1, it is apparent that relatively less $Mn(CO)_5$ is generated upon KrF laser photolysis than is generated upon XeF laser photolysis. Note that since relatively less $Mn(CO)_5$ is generated, the lower frequency band of $Mn_2(CO)_{10}$ at 1993 cm^{-1} appears as a negative feature in Figure 10. In addition, the absorptions at 1975 and ~2018 cm^{-1} are more intense, and a new (weak) absorption at ~1945 cm^{-1} is observed. These results will be discussed after first comparing them to those obtained via ArF laser photolysis.

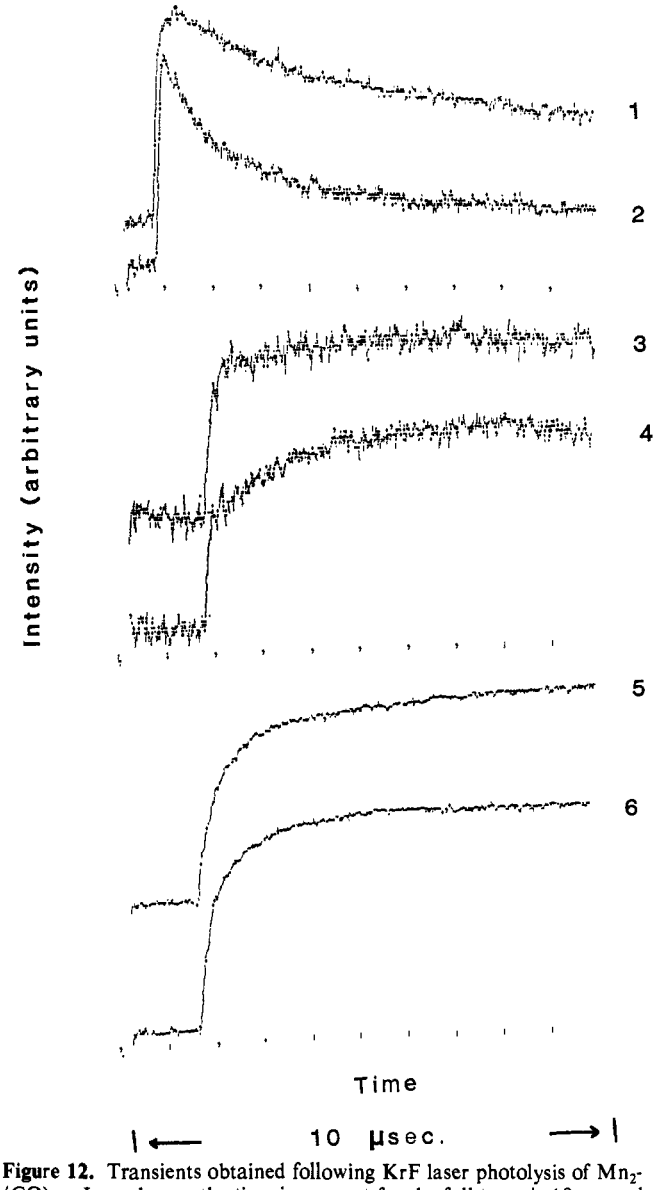

Figure 12. Transients obtained following KrF laser photolysis of $Mn_2(CO)_{10}$. In each case the time increment for the full trace is 10 μs, and all traces were recorded with 15 torr of added argon. In addition, each trace was recorded at the wavelength and with the amount of added CO specified. Trace 1—1972-cm^{-1} probe wavelength with 0.5 torr added CO, trace 2—1972-cm^{-1} probe wavelength with 5.0 torr added CO, trace 3—2018-cm^{-1} probe wavelength with 0.5 torr added CO, trace 4—2018-cm^{-1} probe wavelength with 5.0 torr added CO, trace 5—1999-cm^{-1} probe wavelength with 1.0 torr added CO, and trace 6—1999-cm^{-1} probe wavelength with 7.0 torr added CO.

The transient infrared absorption spectrum 1 μs following ArF laser photolysis of $Mn_2(CO)_{10}$ in the presence of 15 torr Ar is shown in Figure 11. Comparing this spectrum to the KrF laser generated spectrum it is apparent that with ArF laser photolysis even less $Mn(CO)_5$ is generated, the 1975- and 2018-cm^{-1} absorption bands are more intense, the 1945-cm^{-1} band is more intense, and new bands appear at ~1900 and ~1850 cm^{-1}. Also, upon ArF laser photolysis an intense band at ~2048 cm^{-1} is observed. This band, which is presumably *partially* due to "hot" CO (in the $v = 2$ spectral region), is also observed upon KrF laser photolysis.

The observation that there is a decrease in the proportion of $Mn(CO)_5$ generated upon shifting the photolysis wavelength from 351 to 248 cm, and ultimately to 193 nm is consistent with the change in branching ratio ($Mn(CO)_5/Mn_2(CO)_9$) reported by Yasufuku.[13] As formation of $Mn_2(CO)_9$ becomes more favorable the intensity of the transient absorptions at 2018- and 1980-cm^{-1} increases. Since gas-phase $Mn_2(CO)_9$ is expected to exhibit ab-

(27) Levenson, R. A.; Gray, H. B. *J. Am. Chem. Soc.* **1975**, *97*, 6042.

sorptions close to these frequencies, this further confirms that these two features are $Mn_2(CO)_9$ absorptions. However, these absorption bands are, unfortunately, overlapped with those of other species. The 1980-cm^{-1} band, in particular, is overlapped with that of at least one other, as yet, unidentified species. The absorptions at 1945, 1900, and 1850 cm^{-1} in Figure 11 are also unassigned.

The unidentified absorptions are likely to arise from processes such as

$$Mn(CO)_5^{\ddagger} \rightarrow Mn(CO)_4 + CO \quad (5)$$

$$\text{or} \quad Mn_2(CO)_9^{\ddagger} \rightarrow Mn_2(CO)_8 + CO \quad (6)$$

$$\text{or} \quad Mn_2(CO)_9^{\ddagger} \rightarrow Mn(CO)_5 + Mn(CO)_4 \quad (7)$$

where ‡ signifies internal excitation. Since the infrared spectroscopy of species such as $Mn(CO)_x$ and $Mn_2(CO)_y$ ($x < 5$, $y < 9$) have not been studied in a matrix environment, we rely on kinetic evidence in an attempt to distinguish between processes 5, 6, and 7. To distinguish between these alternatives, preliminary measurements of the temporal behavior of the unidentified absorptions as well as those of $Mn_2(CO)_9$ at 2018 cm^{-1} and $Mn(CO)_5$ at 2000 cm^{-1} have been made upon addition of CO to the photolysis cell. While the unidentified bands are observed to decay rapidly upon CO addition (Figure 12, traces 1 and 2), the temporal behavior of the $Mn(CO)_5$ absorption is unaffected (Figure 12, traces 5 and 6). The behavior of the $Mn_2(CO)_9$ absorption, however, does change (Figure 12, traces 3 and 4). From Figure 12, trace 4, it is seen that the rise rate of the absorption has a relatively slow component in addition to the initial rapid rise observed in Figure 12, trace 3. The rapid rise is due to the production of $Mn_2(CO)_9$ in the primary photoprocess. The appearance of the slowly rising component upon CO addition is indicative of formation of $Mn_2(CO)_9$ by reaction of some other species (presumably $Mn_2(CO)_8$) with CO. Thus, we attribute most if not all of the unassigned absorptions in Figures 10 and 11 to $Mn_2(CO)_x$ species. Clearly more work will be necessary to attribute specific absorptions to specific $Mn_2(CO)_x$ species. It is, however, interesting that decarbonylation of $Mn_2(CO)_9$ seems preferable to Mn–Mn bond cleavage in $Mn_2(CO)_9$ or to decarbonylation of $Mn(CO)_5$. This seems to imply that, in agreement with Vaida's results,[15] the Mn–Mn bond strength may *increase* as CO ligands are removed.

Conclusion

Both $Mn_2(CO)_9$ and $Mn(CO)_5$ are primary photoproducts of the UV photolysis of gas-phase $Mn_2(CO)_9$ at 351, 248, and 193 nm. The observation that the branching ratio $Mn(CO)_5/Mn_2(CO)_9$ can be shifted to favor formation of $Mn_2(CO)_9$ by increasing the photolysis frequency is consistent with results of solution phase studies and is interpreted as a change in the relative probability of optically populating the different electronic states from which photochemistry occurs. The infrared absorption spectrum of the $Mn(CO)_5$ and $Mn_2(CO)_9$ transient species has been measured in the gas phase. An intense absorption, centered at 2000 cm^{-1}, which exhibits second-order decay kinetics, has been attributed to two overlapped absorption bands (E and A_1) of C_{4v} $Mn(CO)_5$. This assignment is consistent with results reported for both matrix isolated and solution phase $Mn(CO)_5$ species (Table I). The gas-phase $Mn_2(CO)_9$ species is found to exhibit infrared absorptions at ~2045, ~2018, ~1980, and 1745 cm^{-1}. These results are also consistent with those of solution phase studies (Table I). However, the CO stretch of the bridging carbonyl occurs at an unexpectedly low frequency. The rate constant for the radical–radical recombination reaction has been measured to be $(4.5 \pm 1.0) \times 10^{10}$ L mol^{-1} s^{-1}, which indicates that $Mn_2(CO)_{10}$ is reformed by this pathway with a cross section approaching gas kinetic. The rate constant for the reaction of $Mn_2(CO)_9$ with CO has been measured to be $(2.4 \pm 0.8) \times 10^6$ L mol^{-1} s^{-1}. This $Mn_2(CO)_{10}$ reformation reaction was observed to be relatively slow in solution phase as well ($k = 2.7 \times 10^6$ L mol^{-1} s^{-1} in C_7H_{16}). As was found for $Fe(CO)_x$ and $Cr(CO)_x$ species, the $Mn(CO)_5$ species displays significant internal excitation when formed by UV photolysis.[18,22]

Table I. Infrared Absorptions of $Mn(CO)_5$ and $Mn_2(CO)_9$

compd	medium	absorption freq (cm^{-1})	assignment	ref
$Mn(CO)_5$	CO matrix (20 K)	1993,[a] 1988[a]	E	9
		1978	A_1	
	C_6H_{12} (l)	1990	E & A_1[b]	11
	gas phase	2000	E & A_1[b]	this work
$Mn_2(CO)_9$	Ar matrix (12 K)	2058, 2037, 1993, 1997	T	7b
		1764	B	
	3-methylpentane	2055, 2017, 1986	T	7a
		1760	B	
	C_6H_{12}	2058, 2020, 2006, 1994, 1966	T	11
		1760	B	
	gas phase	~2050, ~2014, ~1980	T	this work
		1745	B	

[a] Matrix split mode. [b] Unresolved bands. T = terminal CO. B = bridging CO.

Acknowledgment. We thank the Air Force Office of Scientific Research for support of this work under Contract 83-0372. We also acknowledge support of this work by the donors of the Petroleum Research Fund, administered by the American Chemical Society. We thank Dr. Martyn Poliakoff and Professor J. J. Turner for some very useful and informative discussions and are grateful for support from NATO which facilitated these discussions.

Registry No. $Mn_2(CO)_{10}$, 10170-69-1; $Mn(CO)_5$, 14971-26-7; $Mn_2(CO)_9$, 86728-79-2; CO, 630-08-0.